

Non Invasive Monitoring of Blood Oxygenation by Phase Resolved Transmission Spectroscopy

A.H. Hielscher^{1,2}, F.K. Tittel² and S.L. Jacques¹

¹University of Texas M.D. Anderson Cancer Center,
Laser Biology Research Laboratory,
Houston, Texas 77030

²Rice University, Department of Electrical
and Computer Engineering,
Houston, Texas 77251-1892

ABSTRACT

A new non invasive method for continuously monitoring the blood oxygenation status, especially in the brain of newborn infants is proposed. This approach is based on measurements of the frequency dependent phase shift and demodulation of intensity modulated near infrared light which is transmitted through the skull. The quantitative determination of hemoglobin as well as deoxygenated hemoglobin in the brain is unlike with currently available devices feasible. The influence of boundary conditions and the skull on the measurements was investigated analytically and with Monte-Carlo simulations.

1. INTRODUCTION

The need for monitoring the blood oxygenation of the brains of newborn infants, in intensive care units, is well recognized. Cerebral injuries due to hypoxia as well as hyperoxia are considered to be the cause of about one third of all deaths in the full term infants [1]. In the preterm infant it is estimated to be the cause of neuro-developmental abnormality in up to two thirds of the survivors [2]. Therefore objective measurement techniques are needed which allow for an oxygen support that is sufficient yet minimal toxic.

The clinical findings of hypoxia (e.g. tachypnea, tachycardia or cyanosis) and hyperoxia (e.g. worsening lung disease from direct oxygen toxicity or retinopathy) are unreliable indicators and may even be completely absent until irreversible damage has occurred [3]. The same critique holds for conventional imaging methods like ultrasound, X-ray, CT or NMR, which can only detect irreversible tissue damages [4]. The "gold standard" assays, arterial blood gas measurement or estimation of oxygen consumption, are invasive, expensive, often painful, and not without risk. In addition, these standard methods only reveal static information about oxygenation at one point in time, rather than continuous measurements over time. What is needed is a technique for non invasive continuously monitoring the oxygenation status of the blood in the brain, which would allow to intervene in time to prevent irreversible damage.

In this paper we will first discuss briefly the possibilities and limitations of two current state of the art methods of non invasively measuring the blood oxygenation with light. This will be followed by a proposal how to overcome the limitations. Technical details of a low cost device will be presented, which is based on measurements of the phase shift ϕ and demodulation M of intensity modulated light transmitted through the brain. Special emphasis is put on the questions how boundary conditions and the skull influence the interpretation of the experimental data. Here results of analytical consideration and Monte-Carlo simulations will be presented.

2. STATE OF THE ART TECHNIQUES

2.1. Absorption measurements

Jöbsis first demonstrated the possibility of detecting near infrared light (~800nm) of only $48\mu\text{Wcm}^{-2}$ in a 6.6nm wide band around 800nm, after it traveled through a brain of 13.3cm diameter [5]. In wavelength region between 700-900 nm, known as therapeutical window, the major absorbing chromophores in the brain are the two blood constituents hemoglobin (Hb) and oxygenated hemoglobin (HbO₂) which delivers the oxygen to the cells. These two absorbers display well known different absorption characteristics [9]. Therefore, with the use of at least 2 wavelength it is in principle possible to determine the two unknowns, the concentration of hemoglobin [Hb] and deoxygenated hemoglobin [HbO₂], with a set of linear equations:

$$A_{\lambda 1} = \{\epsilon_{\text{Hb}\lambda 1} [\text{Hb}] + \epsilon_{\text{HbO}_2\lambda 1} [\text{HbO}_2]\} L_{\lambda 1} \quad (1a)$$

$$A_{\lambda 2} = \{\epsilon_{\text{Hb}\lambda 2} [\text{Hb}] + \epsilon_{\text{HbO}_2\lambda 2} [\text{HbO}_2]\} L_{\lambda 2} \quad (1b)$$

where

A_{λ} := Absorption at wavelength λ .

ϵ := Extinction coefficient [$\text{mM}^{-1}\text{cm}^{-1}$]

L_{λ} := Optical path length at wavelength λ .

Several studies have shown the possibility of monitoring changes in the blood oxygenation in this way [4-8]. However in order to quantify the measurements of the absorption (A), the path length (L) traveled by the photons before they reach the detector must be known. Since tissue is a highly scattering media, L is not simply the distance between light source and detector. Usually L is assumed to be a constant, independent of wavelength, blood concentration, or individuals. However Benaron et. al found that even the path length measured among infants of similar weight and age differ substantially [10]. Since blood itself is a highly scattering media, with a different scattering coefficient then brain [11,12], the total blood volume $V_{\text{tot}} = [\text{Hb}] + [\text{HbO}_2]$ will also affect the path length. Thus devices based on pure absorption measurements can only qualitatively detect changes in the oxygenation status, but fail to give quantitative information.

2.2. Phase shift measurements

Recently Chance et al.[13] introduced a device which measures the phase shift ϕ of sinusoidally intensity modulated light which is transmitted through brain. In the case that the modulation frequency f divided by the speed of light in the tissue c is much larger than the absorption coefficient $\mu_a = (A/L)$ (absorption per unit path length) ($2\pi f/c \gg \mu_a$), one can show that ϕ depends linear on μ_a [14]. Thus the ratio of ϕ at two wavelength equals the ratio of μ_a at two wavelength. From the set of linear equation (1,2), one can easily show that:

$$\frac{\phi_{\lambda 1}}{\phi_{\lambda 2}} = \frac{\mu_{a\lambda 1}}{\mu_{a\lambda 2}} = \frac{\epsilon_{\text{Hb}\lambda 1} + (\epsilon_{\text{HbO}_2\lambda 1} - \epsilon_{\text{Hb}\lambda 1}) Y}{\epsilon_{\text{Hb}\lambda 2} + (\epsilon_{\text{HbO}_2\lambda 2} - \epsilon_{\text{Hb}\lambda 2}) Y} \quad (2)$$

where

$$Y := \frac{[\text{HbO}_2]}{[\text{Hb}] + [\text{HbO}_2]} \quad (3)$$

Y is called the blood oxygen saturation. Therefore this kind of devices can measure quantitatively

the blood oxygen saturation. However, a fatal decrease in the total blood volume V_{tot} , when at the same time Y stays constants remains undetected. Another limitation is that devices available so far are capable of measurements up to 200MHz, which limits their use to cases where $\mu_a \ll 2\pi f/c = (2\pi \cdot 200 \cdot 10^6)/(3 \cdot 10^{10}/1.37) \approx 0.06 \text{ cm}^{-1}$. This may actually be too low for some brain tissues. The way to overcome the mentioned limitations is to determine directly μ_a which would allow the calculation of $[\text{Hb}]$ and $[\text{HbO}_2]$ via eq.(1a,b). How can this be done?

3. PHASE AND DEMODULATION MEASUREMENTS

3.1. Demodulation measurements

μ_a can be found when, besides the phase shift ϕ , the demodulation M defined as:

$$M(f, \mu_a, \mu_s) := \left(\frac{(\text{AC-part of transmission})/(\text{DC-part of transmission})}{(\text{AC-part of input})/(\text{DC-part of input})} \right) = \frac{AC_O/DC_O}{AC_i/DC_i} \quad (4)$$

is measured at a known intensity modulation frequency f . ϕ and M both depend on μ_a and the scattering coefficient μ_s . Thus one gets two equations for two unknowns and the quantitative determination of μ_a would be possible.

Fig. 1 displays M as a function of frequency for different μ_a , calculated with the analytical expression found for an infinite medium[15,16]. (The influence of different boundary conditions on M is discussed in detail in Chapter 4). The major technical problem for a low cost device arises from the fact that M drops from one to zero in a rather narrow frequency band. In order to unambiguously determine μ_a , the light modulation frequency f has to be chosen to be within this narrow band. Inexpensive light modulation and detection devices are only available for frequencies

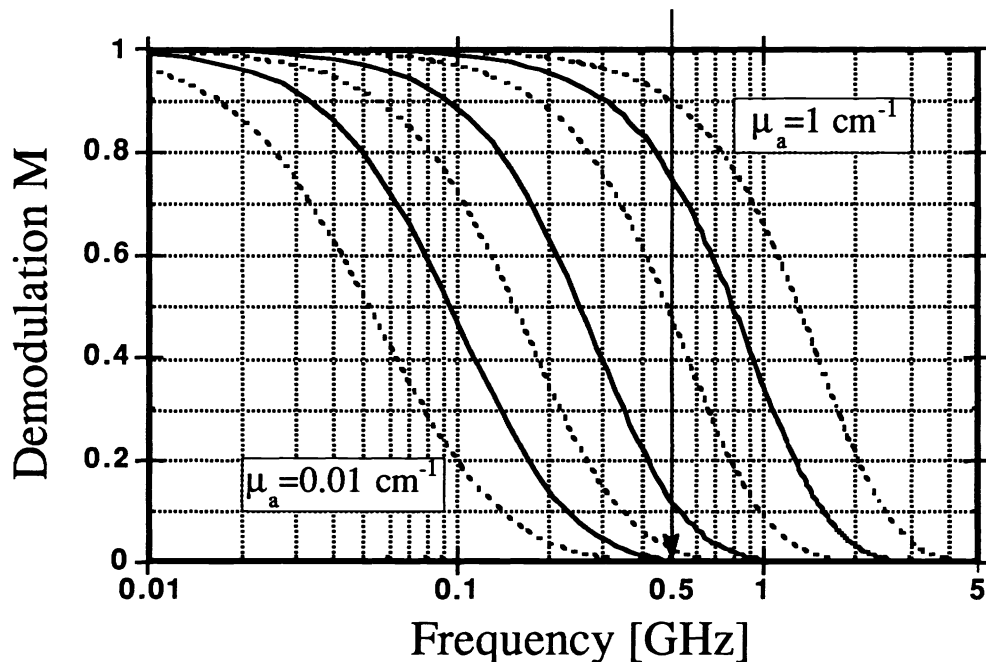


Figure 1: Demodulation M for various absorption coefficient. From left to right $\mu_a = 0.01 \mid 0.025 \mid 0.05 \mid 0.1 \mid 0.25 \mid 0.5 \mid 1 \text{ cm}^{-1}$. Assumed was an infant skull diameter of 10 cm and a typical scattering coefficient of $\mu_s = 5 \text{ cm}^{-1}$ [11,12].

below ~500MHz. Fortunately as fig.1 shows, for typical infant brain tissue with $\mu_a < 0.2 \text{ cm}^{-1}$ [11,12], the demodulation drop occurs indeed below 500 MHz.

3.2 Experimental set up

Fig. 2 displays the experimental set up for a low cost device for the determination of the blood oxygenation in the brain of newborns. Such a device consists out of 5 major parts: 1) the light source and intensity modulation techniques, 2) the light delivery system from the diode to the head of the infant, 3) the light collection and detection, 4) the cross correlation technique for measuring the phase shift ϕ and demodulation M and 5) an algorithm for the determination of $[\text{Hb}]$ and $[\text{HbO}_2]$ from the measured ϕ and M . Points 1-4 will be described in detail in this chapter while part 5 will be addressed in chapter 4.

3.2.1 Light source

As a light source three inexpensive 40 mW Sharp laser diodes (LTO15/17/25MD) provide enough light to probe the brain. The choice of the wavelengths of the laser diodes is determined by the maximum transparency of the brain tissue ($\lambda=700\text{-}900\text{nm}$) and a maximal difference in the extinction coefficient [9]. Thus ideally one would choose $\lambda_1=758\text{nm}$ (maximum of Hb absorption), $\lambda_2=798\text{nm}$ (isobestic point), $\lambda_3=840\text{nm}$ (minimum of Hb absorption). With three wavelengths it is possible to distinguish not only between $[\text{Hb}]$ and $[\text{HbO}_2]$ concentration but also a third unknown background absorption.

In order to intensity modulate laser diodes two components are necessary. First a DC current is set between the lasing threshold current I_{thres} and the maximal allowed current I_{max} . An AC source then has to provide a swing of $\pm(I_{\text{max}} - I_{\text{min}})$. Both signals are added together in a Bias-T (Seastar Optics B.C. Canada), which prevents the rf power to enter the DC current source and vice versa. Modulation depths of >70% for frequencies up to 600 MHz are achievable.

3.2.2 Light Delivery System

In order to bring the light from the diode to the skull, optical fibers are the optimal choice in a clinical environment. So called pick tailed laser diodes are commercially available with an already attached fiber (Seastar Optics, B.C.). Coupling efficiency of up to ~80% are reached. In order to be able to switch between the three wavelengths an optical switch is employed (JDS Fitel, Ontario Canada). These kind of switches align under electro-mechanical control two fiber ends so that maximal transmission is achieved (typ.~90%, when fiber ends are coated). The three diode picktails serve as input fibers to the switch, which has one output fiber which guides the light to the skull. The switching rate between adjacent input channels is about 20ms. An optical switch rather than a direct on and off switching of the laser diodes is preferable, because switching the laser diodes causes intensity and wavelength instabilities. Laser diodes need several minutes to get fairly stabilized. The employment of an optical switch allows the diodes to remain in an operative mode during the change of wavelength for the measurements.

At the interfaces laser diode fiber/optical switch/delivery fiber optical connectors are necessary. A variety of different types are offered [17]. They differ in transfer losses and amount of back reflections. Good connectors allow a transmission of >90% and back reflections smaller than 0.01% (Rifocs, Camarillo, Ca). Backreflection into the laser diode influences the intensity stability and limits the maximal modulation frequency. In order to further reduce back reflections from fiber/fiber and skin/fiber interfaces to the laser diode, optical isolators between laser diodes and fiber would be the optimal solution.

After the switch an optical splitter is needed to bring most of the light (~99.5%) to the skull and a small portion to the reference detector. An easy way to realize such a splitter is to remove the cladding of the "skull-fiber" over a length of ~1cm, place the "reference fiber" adjacent and bend this system slightly. In this way a few modes are coupled out of the "skull-fiber", which yields normally sufficient light for a photomultiplier tube in the reference channel.

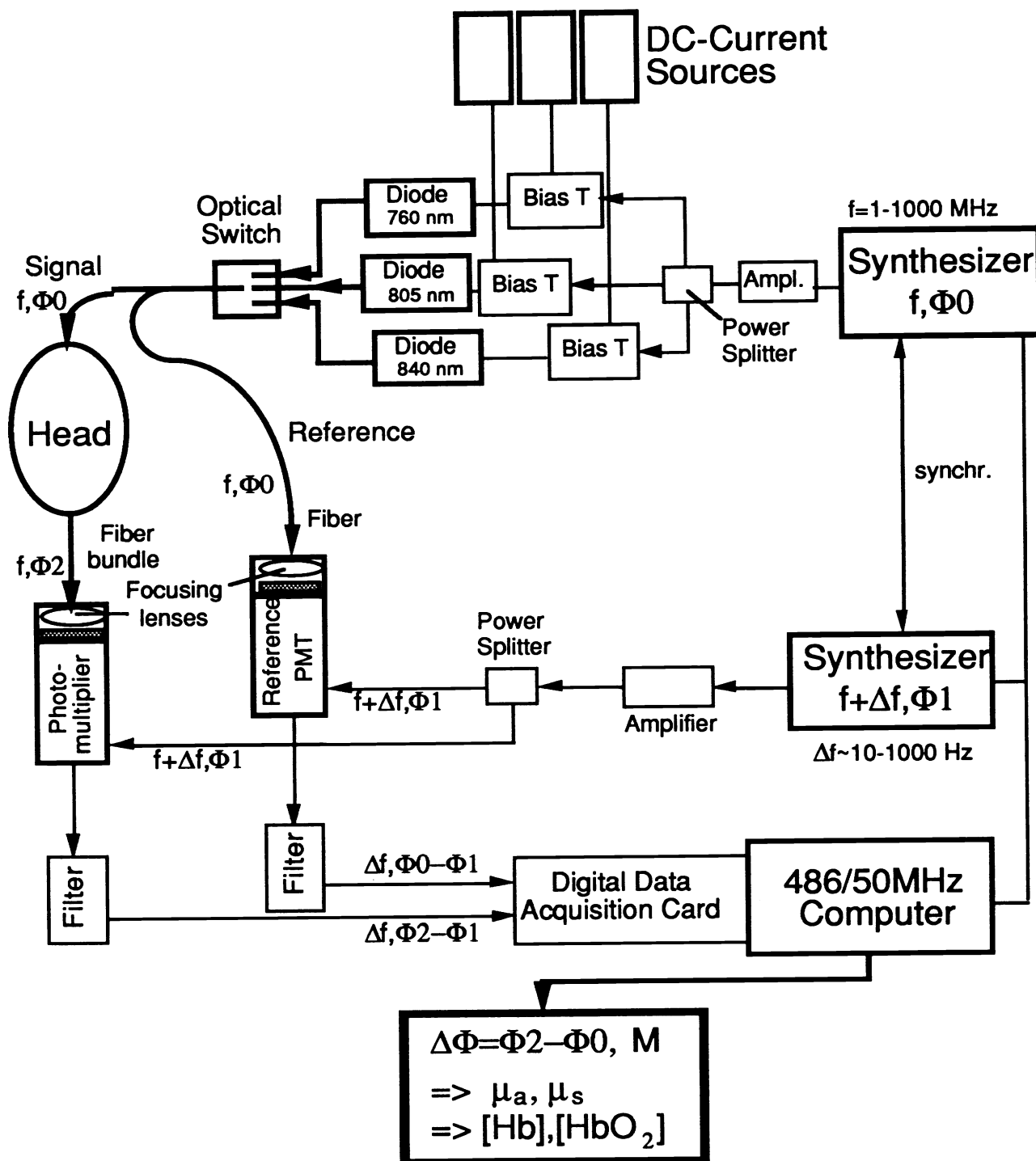


Fig. 2: Experimental set up for cross correlation measurements of the phase shift ϕ and demodulation M .

3.2.3 Light Collection and Detection

The light transmitted through the skull is collected with a fiber bundle (diameter 3.2mm; numerical aperture 0.56). As a light detector two photomultiplier tubes (PMT's) should be used, one to measure the light transmitted through the head, another in a reference channel. PMT's have the necessary sensitivity to detect the extremely weak transmission signals. A multialkali cathode has to be employed in order to obtain the sensitivity beyond a wavelength of 800 nm. Since it was demonstrated chapter 3.1 (Fig.1) that intensity modulation frequencies below 500 MHz suffice for measurements of the oxygenation of the blood in the brain, a R928 Hamamatsu PMT's which cost only ~300\$ can be used, rather than ~12000\$ microchannel plates. This standard laboratory PMT has a time resolution of about 2.5 - 5ns which equals 200-400MHz. However focusing the input light on the cathode to a spot of ~ 1mm diameter has been found to increase the time resolution [18,19]. Thus a special focusing mimic should be provided for optimal time resolution. (e.g.Oriel "77260 x-y-z Lens-Filter-Shutter Assembly").

3.2.4 Cross Correlation Technique

In Fig. 7 the set up for measurements of the phase shift ϕ and demodulation M by means of a cross correlation technique is shown. This well established method [20-23] transforms the cumbersome rf-frequencies of the light modulation into signals in the range below 1 kHz. Measurements of ϕ and M are easy to perform at this low frequencies with accurate digital techniques [24]. One frequency synthesizer (Marconi 2022D) with a frequency $\omega=2\pi f$ is used to intensity modulate the laser diodes, by modulating the drive current of the diode. A second synthesizer with a slightly different frequency $f+\Delta f$ ($\Delta f=10$ -1000 Hz) is used to modulate the gain of the PMT's in the reference and signal channel, by sinusoidally modulating the voltage of the second dynode. In this way the difference frequency Δf between the light source modulation and the gain modulation is generated within the PMT's. The PMT acts as a mixer. The difference frequency in the kHz range can easily be filtered from the rf frequencies by the digital data acquisition system [24]. One can show that these low cross correlation frequencies contain the same phase and modulation information as the rf frequencies [20]. The phase shift can be measured typically within 0.05° and the demodulation within 0.002 [21].

4. DETERMINATION OF OPTICAL PROPERTIES

It is one problem to measure the phase shift ϕ and demodulation M accurately up to 500 MHz. It is another one, at least as important, to determine the right μ_a and thus $[Hb]$ and $[HbO_2]$, given the measured ϕ and M . Basically there are two possibilities: Either an analytical expression is fitted on the phase and demodulation spectrum, or a Newton Raphson algorithm [25] is used to extract μ_a and μ_s from measurements of ϕ and M at one wavelength. For both methods analytical expressions for ϕ and M in dependence of μ_a and μ_s are needed. However analytical expressions for ϕ and M exist only for simple geometries like the infinite or semi-infinite media [26]. For more realistic and thus complicated geometries, analytical expressions based on diffusion approximation to the Boltzman transport equation [27,28] exist only in the time domain [26]. Thus the question arises how large is the error in the μ_a and μ_s values, when the analytical expressions for semi-infinite or infinite media are used in the above mentioned algorithms?

4.1. Influence of boundaries

In order to answer this question the following three systems were compared: infinite medium, semi-infinite medium and a slab (fig.3). For the infinite medium and the semi-infinite medium the phase shift ϕ and demodulation M were calculated with the analytical expression

found from diffusion theory [15,16,26,29] (see also Appendix A). ϕ and M for the slab were determined by numerically computing the Fourier transform of the analytical expression found for the time-domain [26,30]. The result is displayed in fig. 4. It can be seen that in the infinite media a larger ϕ is observed than in the semi-infinite medium, which again yields a larger ϕ than the slab medium. For M this relationship is found in inverse order. This can be explained in the following way: The more boundaries a medium has the more likely it is that photon with a long pathlength escape the medium and are lost for detection. Thus the average pathlength of all photons which reach the detector is decreased. But a decrease in the average pathlength just means a decrease in the measured phase shift, since the photons travel less time in an optical denser medium. For the same reasons the demodulation increases in mediums with more boundaries. We can generalize and say: The larger the ratio of surface divided by volume of a medium, the smaller the observed phase shift and the larger the demodulation.

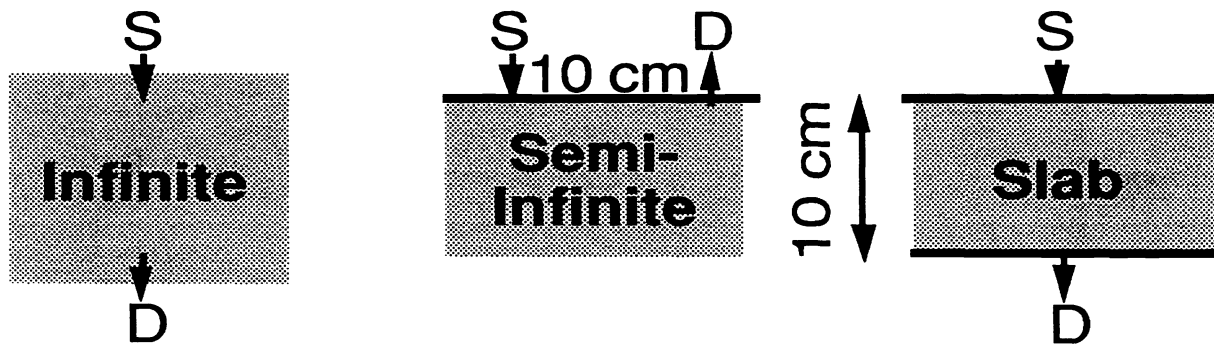


Fig.3: Comparison of three systems. Source S and detector D are 10 cm apart. The optical properties are: $\mu_a=0.1\text{cm}^{-1}$, $\mu_s=5\text{cm}^{-1}$ and $g=0.92$.

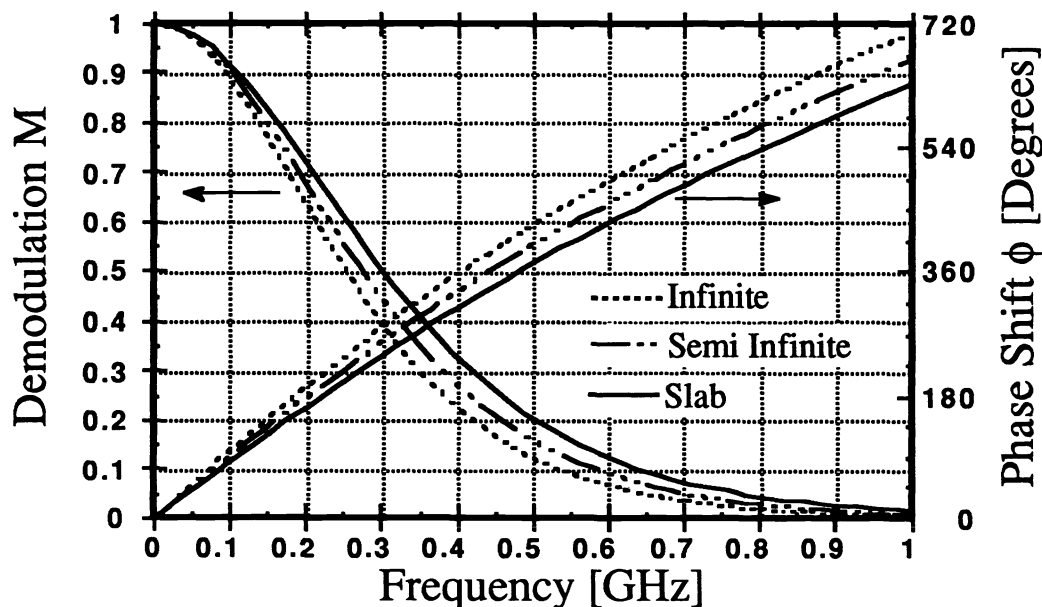


Fig.4: Phase Shift ϕ and demodulation M for different geometries, as depict in fig.3.

In order to quantify the effect in the case of oxygenation measurements of brain tissue we calculated ϕ and M for a set of μ_a and μ_s values which cover the range of optical parameters typically found in brain tissue [12]. In fig.5 it can be seen that with decreasing μ_a , the deviation between semi-infinite medium and slab increases. This can be understood with a similar argument

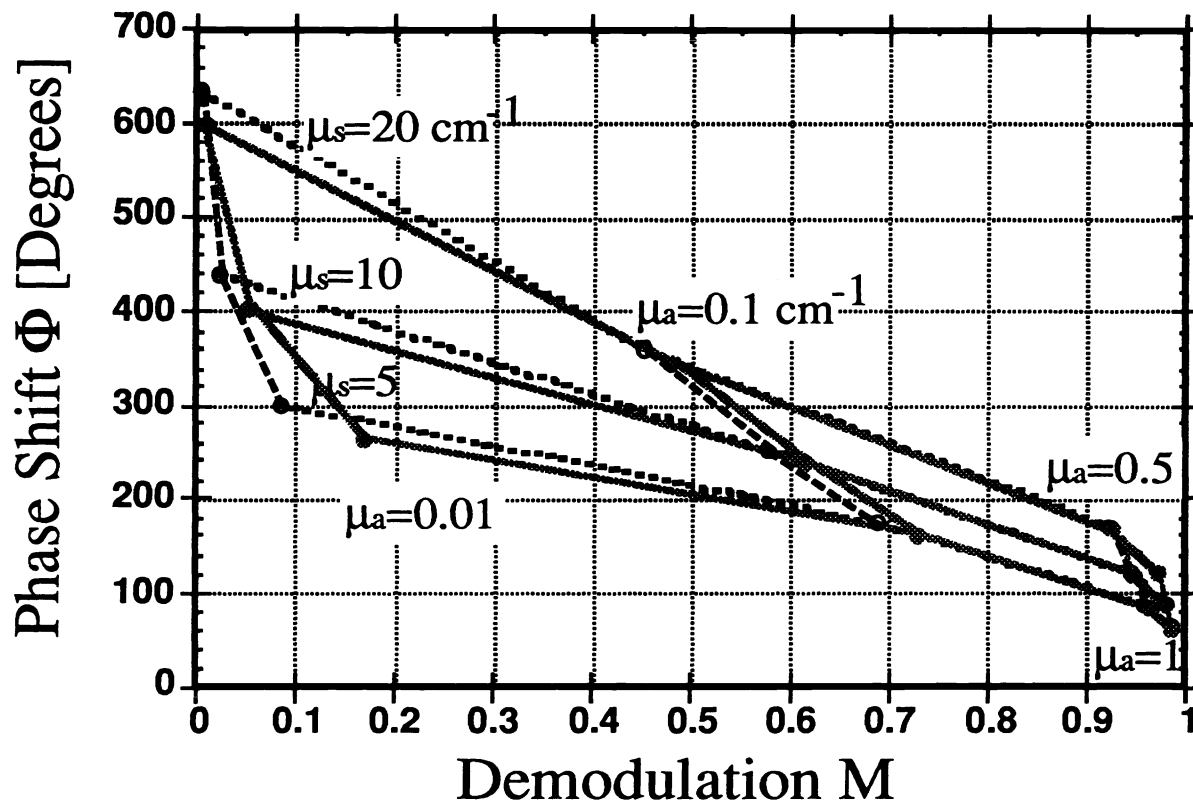


Fig.5: ϕ α $\nu \delta$ M for typical optical parameters found in brain tissue. The intensity modulation frequency is $f=200$ MHz. The distance between source and detector $d=10$ cm. The dashed line grid assumes a semi-infinite medium, the solid line grid assumes a lab geometry (see fig.3). The horizontal lines are iso- μ_s lines while the vertical lines are iso- μ_a lines.

given above. The lower μ_a the more photons from long paths can contribute to the signal. In the slab medium this longer pathlength escape the medium more likely than in the semi-infinite medium. The difference in the mean pathlengths, and thus in ϕ and M , for both systems increases with the increase of photons taking longer pathlength.

The analytical expression given for the semi-infinite medium can be fitted on the data found for the slab medium. This fit gives a new set of μ_a , μ_s values which can be compared with the original values assumed for generating the data for the slab medium. We found that assuming a semi infinite medium instead of a slab leads to an overestimation of μ_a from only 2% in case of $\mu_a=1\text{cm}^{-1}$ to almost 200% for $\mu_a=0.01\text{cm}^{-1}$. Since μ_a depends linear on $[\text{Hb}]$ and $[\text{HbO}_2]$, $[\text{Hb}]$ and $[\text{HbO}_2]$ are effected to the same extend. The scattering coefficients μ_s are much less effected. They are underestimated from $\sim 2\%$ at $\mu_a=1\text{cm}^{-1}$, to $\sim 13\%$ at $\mu_a=0.01\text{cm}^{-1}$.

4.2. Influence of skull

We neglected so far, that the brain is surrounded by a skull with low μ_a . In order to evaluated its influence on measurements of the blood oxygenation the two cases of light transmission through and light reflection from a sandwich like medium were investigated by means of time resolved Monte Carlo simulations. The response to a δ input pulse of three different 1.8 cm slab systems, depict in fig.6, were compared.

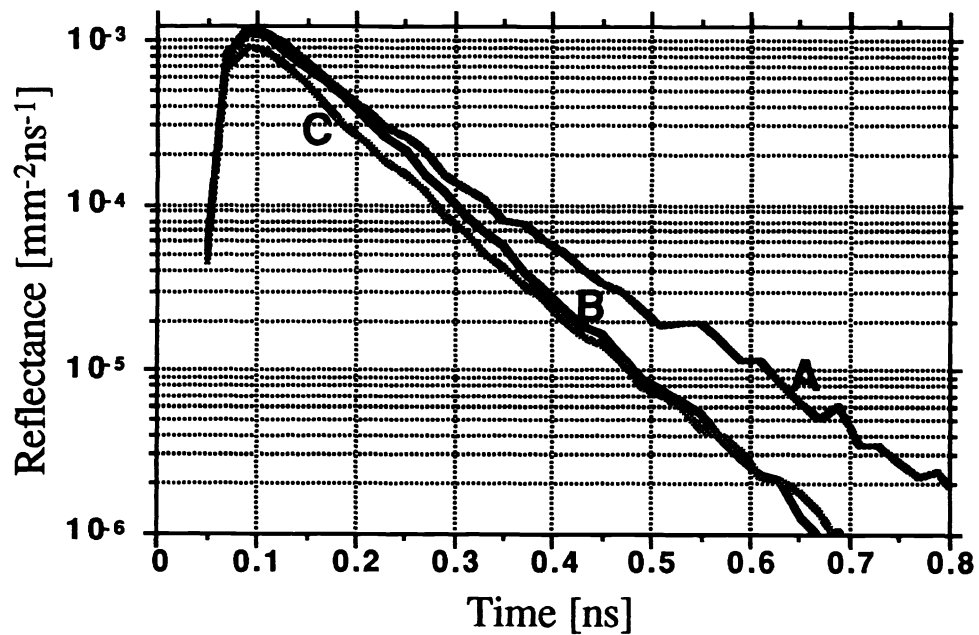
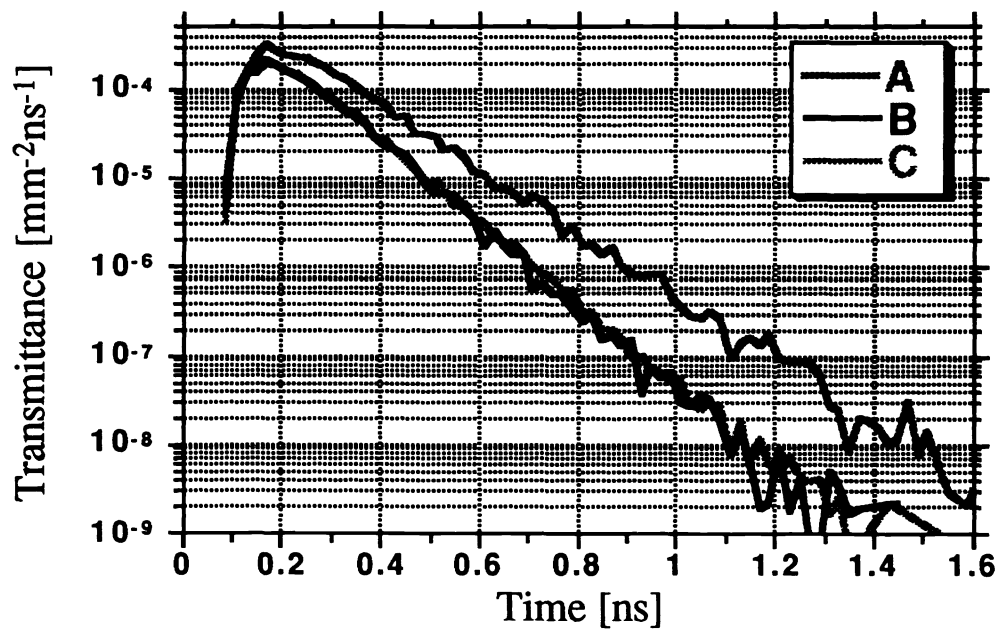
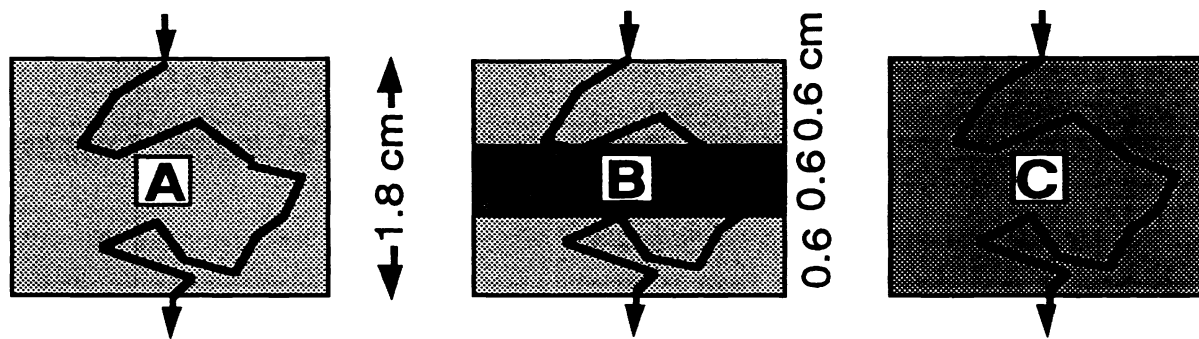


Fig.6(top) / 7(middle) / 8(bottom)

Fig.6 (top fig.): Comparison between (A) homogenous media with $\mu_a=0.2\text{cm}^{-1}$, (B) sandwich like heterogeneous media with $\mu_a=0.2 \mid 0.5 \mid 0.2 \text{ cm}^{-1}$ and (C) another homogenous media with $\mu_a=(0.2+0.5+0.2)/3=0.3\text{cm}^{-1}$. which equals the mean value of absorption coefficients of case (B). The scattering coefficient is $\mu_s=5\text{cm}^{-1}$ in all cases.

Fig.7/8: Time-resolved transmittance (middle fig.)/reflectance (bottom fig.) through a homogenous media and sandwich like heterogeneous media .

The results for transmission measurements are shown in fig.7. As expected the sandwich signal (B) is weaker and decays faster than the signal found for the $\mu_a=0.2\text{cm}^{-1}$ medium (A). However it turns out, that the transmission signal found for the sandwich structure can not be distinguished from the signal found for the homogenous medium with the in average increased μ_a (C). If we assume a skull of 2.5mm thickness surrounding a typical infant brain of a diameter of 9.5 cm, one will underestimate μ_a and thus the concentrations of the blood constituents [Hb] and [HbO₂] by maximal 5%.

Are the measurements performed on the same systems, but in reflection, with the source and detector separated by 1 cm on the surfaces of the slabs, a different behavior evolves (fig.8). One can observe that in this case the time-resolved signals of the homogenous medium (A) and the sandwich medium (B) equal during the first 200ps. After that the two curves depart and the sandwich structure signal approaches the curve of the homogenous medium (C). The early photons obviously do not travel deep enough to be affected by the higher absorbing layer in 6mm depth of the sandwich. Other than with transmission measurements, do measurements of the time resolved reflectance allow for a characterization of multi-layered systems. The time of departure can be used for layer depth resolution, while the strength of the decay is indicative of the absorption coefficient of the lower layer. More work has to be done to quantify these kind of measurements (see also [31,32]).

5. SUMMARY

Most of the problems in the infant intensity care arise from inappropriate oxygen supply of the brain. Currently available devices can detect qualitatively changes in the concentration of hemoglobin [HbO] and deoxygenated hemoglobin [HbO₂] (absorption measurements) or blood oxygen saturation levels (phase resolved measurements). However, these methods do not provide quantitative information about [Hb], [HbO₂] and the total blood volume $V_{\text{tot}}=[\text{Hb}]+[\text{HbO}_2]$. These values can be gained by measurements of the phase shift ϕ and demodulation M of light trans-mitted through the brain. Because in infant brain tissue it is expected that the demodulation drops from one to zero well below 500MHz, low cost devices based on inexpensive laser diodes and photomultiplier tubes, are feasible.

Only for infinite and semi infinite mediums analytical expressions for the phase shift ϕ and demodulation M in dependence of μ_a and μ_s (and therefore in dependence of the concentrations of [Hb] and [HbO₂]) exist. When they are used in algorithms for the determination of μ_a from ϕ and M measurements on "real" systems with a more complicated geometry, the blood concentration is at least overestimated from 2% two 180%, depending on the concentration of the blood constituents. The lower the concentration the stronger the overestimation. The influence of the skull on oxygenation measurements leads in the case of transmission measurements to an underestimation of the concentrations below 5%. Reflection measurements can be used to analyze the structure of multi-layered tissue, e.g. the determination of the skull thickness.

6. ACKNOWLEDGMENT

This work was supported in part by the Department of Energy. The authors would like to thank M. vandeVen and B. Barbierie from ISS in Urbana/Champaign, IL., for the fruitful discussions concerning the design of the phase/modulation measurement device.

7. APPENDIX

In this appendix it will be shown that the two quit different looking expressions for the phase shift and demodulation found currently in literature are actually equivalent. The expressions given by Fishkin et al [16], includes trigonometric functions while Tromberg et al [15], succeed in deriving an expression without these computational cumbersome functions. The difference in the appearance of the formulas stems from the different way both groups solve the AC-part of the diffusion approximation to the Boltzman Transport equation. This approximation leads to the following equation [15,30]:

$$\frac{1}{c} \frac{\partial \Psi(\mathbf{r}, t)}{\partial t} - D \nabla^2 \Psi(\mathbf{r}, t) + \mu_a \Psi(\mathbf{r}, t) = S(\mathbf{r}, t) \quad (\text{A1})$$

where Ψ is the fluence rate, $D = (3(\mu_a + (1-g)\mu_s))^{-1}$ is the diffusion constant and S the source term. If S is an AC-point source which emits sinusoidally modulated radiation at a frequency $\omega = 2\pi f$ ($S(\mathbf{r}, t) = \delta(\mathbf{r}) S_0 \exp(i\omega t)$), we can assume a spherical symmetric solution of the form :

$$\Psi(\mathbf{r}, t) = \frac{\Psi(r)}{r} \exp(-i\omega t) \quad (\text{A2})$$

Inserting (A2) into (A1) yields:

$$\frac{\partial^2 \Psi(r)}{\partial r^2} - \left(\frac{\mu_a}{D} + i \frac{\omega}{cD} \right) \Psi(r) = \frac{S_0}{D} \delta(r=0) \quad (\text{A3a})$$

or

$$(\partial^2 / \partial r^2) \Psi(r) - k^2 \Psi(r) = \frac{S_0}{D} \delta(r=0) \quad (\text{A3b})$$

with

$$k = \sqrt{\left(\frac{\mu_a}{D} + i \frac{\omega}{cD} \right)} = \sqrt{a + ib} \quad (\text{A4})$$

Equation (A3b) resembles the well known Helmholtz equation, only that usually k is not considered complex. If one requires, that the fluence rate Ψ is limited for $r \rightarrow \infty$, the solution for this equation for $r \neq 0$ can be expressed in the form

$$\Psi(r) = \Psi_1 \exp(-kr) \quad (\text{A5})$$

Depending now on how the complex k in the exponent is handled, one reaches to either the expression given by Fishkin et al. or the Tromberg et al. . k can be transformed in two ways: Either one uses like Tromberg et al. the equality

$$\sqrt{a+ib} = \sqrt{\frac{a + \sqrt{a^2 + b^2}}{2}} + i \sqrt{\frac{-a + \sqrt{a^2 + b^2}}{2}} \quad (\text{A6}),$$

or one uses like Fishkin et al. , the equality

$$\sqrt{a+ib} = i\sqrt{A\exp(i\phi)} \quad , \quad \text{with } A=\sqrt{a^2+b^2} \text{ and } \phi=\tan^{-1}(b/a) \text{ this yields:}$$

$$\sqrt{a+ib} = \sqrt{\sqrt{a^2+b^2}} e^{i 1/2 \phi} = \sqrt{\sqrt{a^2+b^2}} \{ \cos [1/2 \tan^{-1}(b/a)] + i \sin [1/2 \tan^{-1}(b/a)] \} \quad (A7)$$

After substituting back for a,b (see eq.(A4) and D into (A6) and inserting the result into equation (A5), one finds the AC-part of the Tromberg et al. expression for the radiant energy fluence:

$$\begin{aligned} \Psi = \Psi_{AC}(r,t) = \frac{\Psi_1}{r} \exp\{-r\sqrt{3/2\mu_a(\mu_a+\mu_s)} \sqrt{\sqrt{1+(\frac{\omega}{\mu_a c})^2} + 1} \} \\ * \exp\{i r\sqrt{3/2\mu_a(\mu_a+\mu_s)} \sqrt{\sqrt{1+(\frac{\omega}{\mu_a c})^2} - 1} \} * \exp(-i \omega t) \quad (A8) \end{aligned}$$

If equality (A7) is used to transform k, rather than (A6) we get instead:

$$\begin{aligned} \Psi_{AC}(r,t) = \frac{\Psi_1}{r} \exp\{-r \sqrt{\sqrt{\frac{c^2\mu_a^2+\omega^2}{c^2D^2}} \cos(1/2 \tan^{-1}(\frac{\omega}{\mu_a c}))} \} \\ * \exp\{-i r \sqrt{\sqrt{\frac{c^2\mu_a^2+\omega^2}{c^2D^2}} \sin(1/2 \tan^{-1}(\frac{\omega}{\mu_a c}))} \} * \exp(-i \omega t) \quad (A9) \end{aligned}$$

which equals exactly the expression given by Fishkin et al. Thus the expression given by Tromberg et al. and Fishkin et al. can be transformed in each other by using the equalities:

$$\sqrt{\frac{1 + \frac{1}{\sqrt{1+(\omega/\mu_a c)^2}}}{2}} = \cos [1/2 \tan^{-1}(\omega/\mu_a c)] \quad (A10a)$$

and

$$\sqrt{\frac{1 - \frac{1}{\sqrt{1+(\omega/\mu_a c)^2}}}{2}} = \sin [1/2 \tan^{-1}(\omega/\mu_a c)] \quad (A10b)$$

which follow directly from (A6) and (A7). The phase shift ϕ is just given by the expressions in the imaginary exponent of (A8) and (A9). The demodulation is defined in the text (eq.4)

Even though Fishkins et al. and Trombergs et al. expressions are mathematically the same, one has to be careful while using them in programming. It is necessary to use double precision variables in order to avoid deviations in the calculations of both expressions. Furthermore avoiding trigonometric function in mathematical algorithms (e.g. fitting routines) can decrease the computation time drastically and increase the region of convergence (e.g. Newton Raphson).

8. REFERENCES

- [1] Pape K.E., Wigglesworth J.S., "Haemorrhage ischaemia and the prenatal brain", Heinemann Medical Books (London) for *Spastics Int. Med. Publ.* (1979)
- [2] Stewart A.L., Thorburn R.J., Hope P.L., Goldsmith M., Lipscomb A.P., Reynolds E.O.R., "Ultrasound appearance of the brain in very preterm infants and neuro-developmental outcome at 18 months of age", *Archives of Disease in Childhood* **58**, 598 (1983)
- [3] Benaron D.A., Benitz W.E., Ariagno R.L., Stevenson D.K., "Noninvasive Methods for Estimating In Vivo Oxygenation", *Clinical Pediatrics* **31**, 258 (1992)
- [4] Cope M., Delpy D.T., "System for long-term measurement of cerebral blood and tissue oxygenation on newborn infants by near infrared transillumination", *Medical and Biological Engineering and Computing* **26**, 289 (1988).
- [5] Jöbsis F.F., "Noninvasive Infrared Monitoring of Cerebral and Myocardial Oxygen Sufficiency and Circulatory Parameters", *Science* **19**, 1264 (1977)
- [6] Thorniley M., Livera L., Wickramasinghe Y., Spencer S.A., Rolfe P., "The non invasive monitoring of cerebral tissue oxygenation", *Adv. in Exp. Med. Biol.* **277**, 323 (1990)
- [7] Tamura T., Eda H., Takada M., Kubodera T., "New Instrument for Monitoring Hemoglobin Oxygenation", *Adv. in Exp. Med. Biol.* **248**, 103-107 (1990)
- [8] Chance B., Leigh J.S., Miyake, H., Smith D.S., Niola D.S., Greenfield R., Finander M., Kaufmann K., Levy W., Young M., Chen P., Yoshioka P., Boretsky R., "Comparison of time Resolved and Unresolved Measurements of Deoxyhemoglobin in Brain", *Proc. National Academy of Science* **85**:4971 (1988)
- [9] Wray S., Cope M., Delpy D.T., Wyatt J.S., Reynolds E., "Characterization of the near infrared absorption spectra of cytochrome aa₃ and haemoglobin for the non-invasive monitoring of cerebral oxygenation", *Biochimica et Biophysica Acta* **933**, 184 (1988)
- [10] Benaron D.A., Gwiazdowski S., Kurth C.D., "Optical path length of 754 nm and 816 nm light emitted into the head of infants", *Proc. IEEE Eng. Med. Biol.* 1990; 3, p.1117
- [11] Duck F.A., "Physical Properties of Tissue", Academic Press, San Diego, Ca (1990)
- [12] Svaasand L.O., Ellingsen R., "Optical Properties of Human Brain", *Photochem. and Photobiol.* **38**, 293 (1983)
- [13] Weng J., Zhang M.Z., Simons K., Chance B., "Measurements of Biological Tissue Metabolism Using Phase Modulation Spectroscopic Technology", SPIE 1431: Time-Resolved Spectroscopy and Imaging of Tissues, 161-170, Los Angeles, Ca (1991).
- [14] E.M. Sevick, B.Chance, J.Leigh, S. Nioka, M. Maris, "Quantitation of Time- and Frequency-Resolved Optical Spectra for the Determination of Tissue Oxygenation", *Analytical Biochemistry* **195**, 330-351 (1991)
- [15] Tromberg B.J., Svaasand L.O., Tsay T.T., Haskell R.C., "Properties of photon density waves in multiple-scattering media", *Applied Optics* **32**, pp. 607-616 (1993)
- [16] Fishkin J., Gratton E., "Propagation of photon density waves in strongly scattering media containing an absorbing semi-infinite plane bounded by a straight edge", *Journal of the Optical Society of America A* **10**, 127-140 (1993)
- [17] Rogers G., Berrang P., "The Pros and Cons of Single-Mode Connectorized Laser Diodes", *Photonic Spectra* Oct. 1991
- [18] Canonica S., Forrer J., Wild U.P., "Improved timing resolution using small side-on photomultipliers in single photon counting", *Rev. Sci. Instrum.* **56**, 175 (1985)
- [19] Personal Communica. with B. Barbierie and M. Van de Veen from ISS, Urbana-Champaign.
- [20] Spencer R.D., Weber G., "Measurement of Subnanosecond Fluorescence Lifetimes with a Cross-correlation Phase Fluorometer", *Ann.N.Y.Academy of Science* **158**,361 (1969)

- [21] Gratton E., Limkeman M., "A continuously variable frequency cross-correlation phase fluorometer with picosecond resolution", *Biophys. J.* **44**, 315 (1983)
- [22] Lakowicz J.R., Maliwal B.P., "Construction and performance of a variable-frequency phase-modulation fluorometer", *Biophys. Chem.* **21**, 61 (1985)
- [23] Laczko G., Gryczynski I., Gryznski Z., Wiczek W., Malak H., Lakowicz J.R., "A 10-GHz frequency-domain fluorometer", *Rev. Sci. Instr.* **61**, 2331 (1990)
- [24] Feddersen B.A., Piston D.W., Gratton E., "Digital parallel acquisition in frequency domain fluorimetry", *Rev. Sci. Instr.* **60**, 2929 (1989)
- [25] Press W.H., Flannery B.P., Teukolsky S.A., Vetterling W.T., "Numerical Recipes in C", Cambridge University Press, New York, NY (1990)
- [26] Arridge S.R., Cope M., Delpy D.T., "The theoretical basis for the determination of optical pathlengths in tissue: temporal and frequency analysis", *Phys. Med. Biol.* **37**, 1531-1560 (1992)
- [27] Case K.M., Zweifel P.F., "Linear Transport Theory", Addison-Wesley, Reading, Massachusetts 1967
- [28] Ishimaru A., "Wave Propagation in Scattering Media", Vol.1, Acad. Press, San Diego, Ca 1978
- [29] Patterson M.S., Moulton J.D., Wilson B.C., Berndt K.W., Lakowicz J.R., "Frequency domain reflectance for the determination of the scattering and absorption properties of tissue", *Applied Optics* **30**, 4474 (1991)
- [30] Patterson M.S., Chance B., Wilson B.C., "Time resolved reflectance and transmittance for the non-invasive measurement of tissue optical properties", *Applied Optics* **28**, 2331 (1989)
- [31] Jacques S.L., Hielscher A.H., Wang L.H., "How surface boundaries and subsurface objects affect time-resolved and phase/modulation-resolved photon migration", see this issue of SPIE proceedings.
- [32] Graber H.L., Barbour R.L., Lubowsky J., Harrison R., Das B.D., Wu K.M., Alfano R.R., "Evaluation of steady state-, time- and frequency-domain data for the problem of optical diffusion tomography", *SPIE 1641: "Physiological Monitoring and Early Detection Diagnostic Methods"*, p.6-20 (1992).